Structural Engineering and Mechanics, Vol. 44, No. 6 (2012) 763-774
DOI: http://dx.doi.org/10.12989/sem.2012.44.6.763

Experimental work on seismic behavior of various types of masonry infilled RC frames

I. Serkan Misir[a], Ozgur Ozcelik*, Sadik Can Girgin[b] and Serap Kahraman[c]

Department of Civil Engineering, Faculty of Engineering, Dokuz Eylul University, 35160, Izmir, Turkey

(Received December 6, 2011, Revised September 18, 2012, Accepted November 8, 2012)

Abstract. Reinforced concrete frame structures with masonry infill walls constitute the significant portion of the building stock in Turkey. Therefore it is very important to understand the behavior of masonry infill frame structures under earthquake loads. This study presents an experimental work performed on reinforced concrete (RC) frames with different types of masonry infills, namely standard and locked bricks. Earthquake effects are induced on the RC frames by quasi-static tests. Results obtained from different frames are compared with each other through various stiffness, strength, and energy related parameters. It is shown that locked bricks may prove useful in decreasing the problems related to horizontal and vertical irregularities defined in building codes. Moreover tests show that locked brick infills maintain their integrity up to very high drift levels, showing that they may have a potential in reducing injuries and fatalities related to falling hazards during severe ground shakings.

Keywords: engineered infills; locked brick masonry infill; reinforced concrete frames; cyclic testing; experimental methods; earthquake engineering

1. Introduction

The most common type of structural system in Turkey for both residential and commercial buildings is multi-storey reinforced concrete frames with masonry infills; therefore it is very important to understand the seismic behavior of these structures under seismic actions. The great deal of research work has been done on the masonry infilled reinforced concrete frames in the last several decades. Effect of masonry infill walls on the dynamic response of reinforced concrete frames is still a subject matter that researchers around the world have been discussing (Pujol and Fick 2010). Dynamic behavior of infilled frames with openings is another debatable topic, and not many analytical and experimental studies on this type of frame have been conducted (Mondal and Jain 2008, Kakaletsis 2009, Tasnimi and Mohebkhah 2011). Dolsek and Fajfar (2001) states that infill walls may have beneficial effects on the dynamic response given that they do not impose irregularities, and do not cause shear failures on the columns. Researchers also suggested that RC frames with unreinforced masonry infills results in larger energy dissipation capacity and increasing

*Corresponding author, Assistant Professor, E-mail: ozgur.ozcelik@deu.edu.tr
[a]Researcher
[b]Research Assistant
[c]Professor

strength and stiffness than similar frames without masonry infill walls (Klingner and Bertero 1976, Santhi *et al.* 2005, Hashemi and Mosalam 2006). Although in general not taken into account during design phases, infill walls increase considerably the lateral stiffnesses of buildings. This in turn increases the frequency content of floor accelerations, therefore infill walls would have a negative impact on the acceleration sensitive non-structural elements whereas due to increase in lateral stiffness, infill walls would have a positive impact on the displacement sensitive non-structural components under moderate earthquakes. Post-earthquake observations of infilled RC frames reveal that infill walls have led to the collapse of buildings due to the masonry infill arrangements creating stiffness discontinuities (Sezen *et al.* 2003). Past research work has shown that the masonry infill walls induce significant change in the seismic response of RC frames. Effects of masonry walls can, in general, be positive meaning that these walls increase overall stiffness and strength of RC frames. On the negative side, masonry infill walls may induce undesired torsional motion by imposing in-plan irregularities and soft-storey and short column effects by imposing vertical irregularities. Some nonlinear modeling efforts to examine nonlinear behavior of infilled reinforced concrete frames based on experimental work are summarized in the literature (Perera *et al.* 2004, Dolsek and Fajfar 2005, Lagaros and Geraki 2008, Talaat and Mosalam 2009). Aref and Jung (2003) tested full scale steel frames infilled with polymer matrix composite (PMC) walls and PMC infilled walls contributed 65% energy dissipation capacity to the steel frames without showing significant degradation in strength and stiffness. Experimental studies investigating the seismic response of infilled RC frames show that brittle damage is observed starting at 1% drift. For improving the seismic behavior of these frames, “engineered infills” have been proposed in the literature in order to change failure modes from brittle failure to sliding failure, which is documented to be more ductile. Mohammadi and Akrami (2010) describes engineered infills as they are expected to have a well-defined strength level, sufficient ductility comparable to other engineered structural elements, stable post peak behavior and high stability in out-of-plane direction during earthquakes comparable to other structural elements. Test specimens in this study were 1/3 scale steel frames infilled with fibrous concrete walls incorporating frictional sliding fuses at their mid-heights. Results showed that by using fuse elements, strength and deformation characteristics of the infilled frames were greatly improved. Mohammadi and Akrami (2011) in another experimental work tested six single-story single-bay steel frames with different fuse configurations in two stages. Results showed that engineered infills with frictional sliding fuses can be considered to have high ductility, transversal stability and sufficient desired strength.

In this paper, the results of a recently conducted experimental work are presented. Experimental program include three half-scale RC frames with three different infill conditions, namely no infill, infill with standard bricks, and infill with a patented new type brick called “locked bricks”. Seismic loads are induced on the specimens by imposing drift in a cyclic quasi-static manner by a displacement controlled actuator (ACI 374.1-05 2005). Results obtained from different frames are compared with each other through various stiffness, strength, and energy related parameters. It is shown that the new locked brick brings the advantage of reducing the undesired effects of vertical irregularities in reinforced concrete structures.

2. Experimental studies

For the experimental work, three one bay-one storey half-scale RC frame specimens were

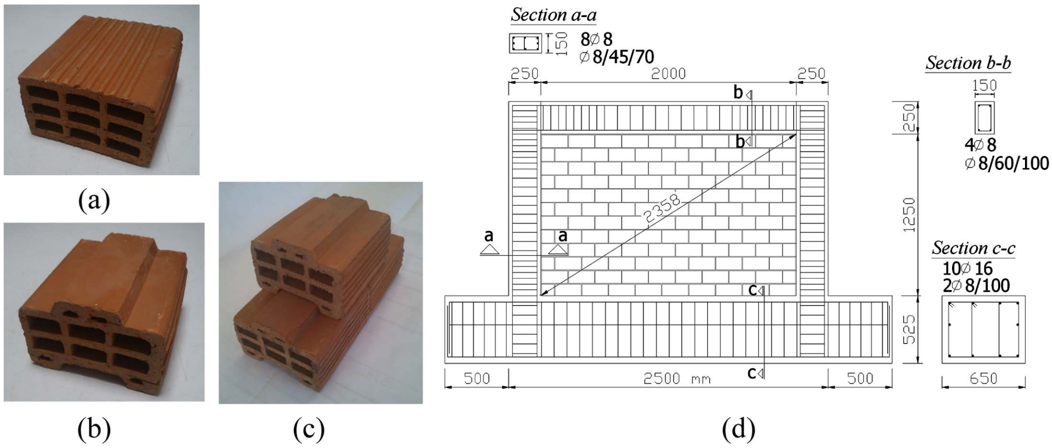

Fig. 1 (a) Standard brick units, (b) locked brick units, (c) placement of locked bricks, and (d) dimensions (mm) and reinforcement details of the specimens

designed according to the Turkish Earthquake Code (Ministry of Public Works and Settlement 2007). All tests were carried out (Ugurlu 2011) in Dokuz Eylul University Civil Engineering Department, Structural Mechanics and Earthquake Engineering Laboratory. Dimensions of standard and locked bricks shown in Fig. 1(a) and Fig. 1(b) are $115 \times 120 \times 65$ mm and $120 \times 125 \times 67.5$ mm and have void ratios of 0.436 and 0.441, respectively. Bricks used for the tests were specifically produced in order to fit the half-scale frame specimens. Locked bricks do not use mortars between brick layers as shown in Fig. 1(c), therefore are significantly differing from standard bricks in terms of the way they are used for constructing infill walls. During the placement of locked brick wall inside the frame, mortars are used only under the first layer and above the last layer of bricks to obtain the out-of-plane stability; no mortar is used on the side close to the frame to avoid shear interaction between the wall and the columns. For the rest of the paper, frames with standard bricks, locked bricks, and with no bricks will be denoted as SBF, LBF, and BaF, respectively. BaF specimen is the control specimen used to investigate the effects of different types of bricks. For all the specimens, plaster with approximately 1.5 cm thickness is used; the plaster and the mortar used for the specimens have the same mix proportions.

2.1 Description of test specimens

The specimens were cast at a precast concrete facility and were transported to the lab, and infill walls were constructed in the lab. Although the equipment and laboratory constraints as well as funding amount limited the sizes of specimens being tested, dimensions and design of test frames were kept as realistic as possible to ensure that the experimental results would be applicable on the real world structures. The dimensions and the reinforcement details of test frames are shown in Fig. 1(d). The amount of steel bars used for the columns and beam are 8Φ8 and 4Φ8, respectively. It is noted here that confinement reinforcements were used in the beam-column connections which is required by the Turkish Earthquake Design Code (2007). Concrete with a maximum diameter of 10 mm for coarse aggregate was used. The material tests both for concrete and reinforcement steel were conducted to characterize the materials used for the test. The effective compressive strength of

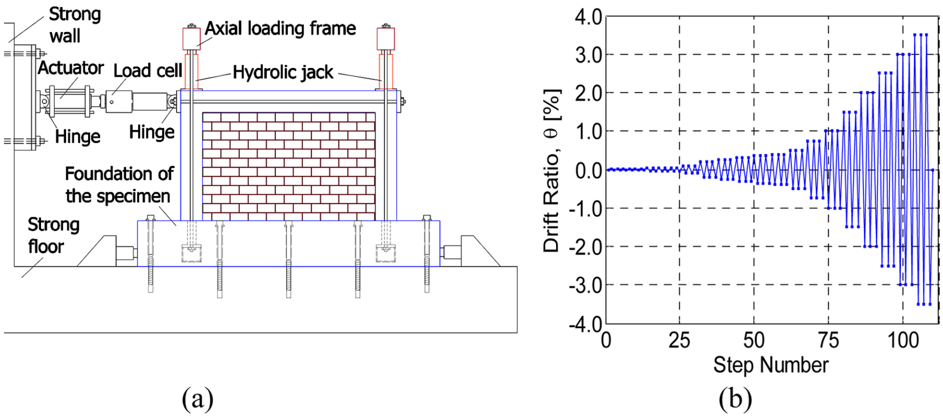

Fig. 2 (a) The test setup and (b) loading protocol

concrete was measured 20 MPa, and the yield and ultimate stresses of reinforcing steel were measured 472 MPa and 538 MPa, respectively. The dimensions of the foundation were 3000 mm in length, 550 mm in width, and 500 mm in height.

2.2 Testing equipment

During the test, a displacement-controlled hydraulic actuator with 300 kN tension/compression capacity is used to enforce specimens to follow a predetermined displacement trajectory while axial loads on each column kept constant by a manually-controlled hydraulic system including hydraulic jacks of 600 kN capacity shown in Fig. 2(a). One end of the hydraulic actuator was attached at the top of one of the columns of the test specimen and the other end was attached to a strong wall. In order to apply the lateral loads evenly to both of the columns, the actuator was attached to the columns' top by using two post-tensioned rods producing approximately 50 kN axial force on the beam. Five vertical rods and two stoppers acting along lateral direction are used to fix the foundation of the specimen to the strong floor.

2.3 Lateral loading protocol

Displacement loading protocol was determined according to ACI 374.1-05 (ACI 374 2005). Under constant axial load of 10% of column axial load capacity, the specimens were subjected to lateral displacement cycles as shown in Fig. 2(b).

2.4 Instrumentation details

In order to monitor the response of the specimens, 29 channels were used in total. Among these channels, a load cell was used to measure the induced lateral force, 16 strain gauges at various locations were used to monitor deformations at critical sections shown in Fig. 3(a), 10 displacement transducers and 2 string-pots were used to monitor the overall deformations of the specimens. Out of plane displacements and foundation movements in the rocking and lateral directions were also monitored during the tests by placing displacement transducers to the appropriate locations. A

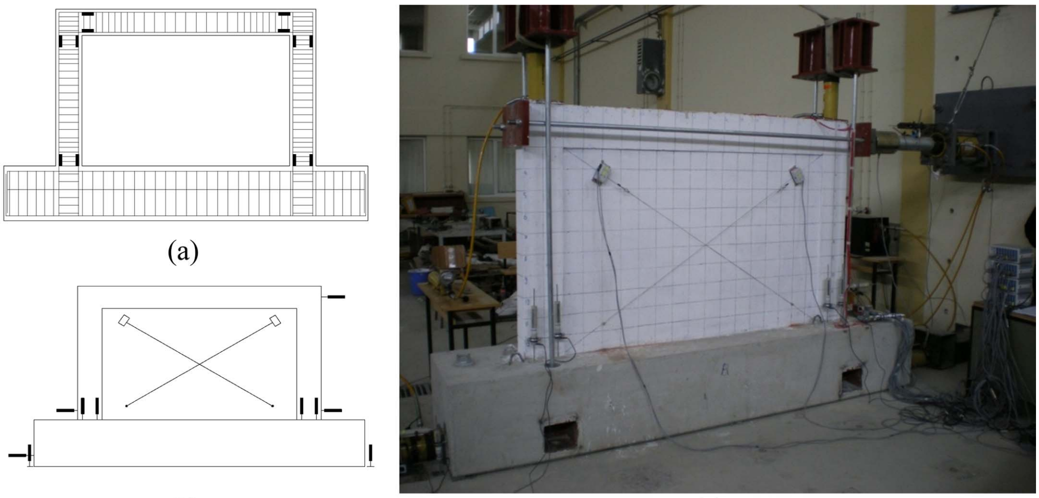

(a)

(b) (c)

Fig. 3 Locations of (a) strain gauges, (b) displacement transducers, and (c) a test specimen prior to a test

representative instrumentation layout, and a test specimen with instruments installed prior to a test are shown in Fig. 3(b) and Fig. 3(c), respectively. Data acquisition hardware used to record the data is a 16 bit system. Each channel was recorded simultaneously with a sampling rate of 8 Hz. The sampling rate chosen was deemed enough since the tests conducted were quasi-static tests.

3. Experimental results

Total of eighteen target displacement cycles with three full cycles at each target displacement were imposed to the frames in each test. In all the tests, the applied maximum story drift was 3.5%. In the following sections some general and detailed observations regarding the results are presented.

3.1 Bare frame (BaF)

Bare frame specimen was taken as the benchmark frame in order to compare its response with respect to its infilled counterparts. The first cracks related to flexural behavior were observed at a story drift of 0.28%. The applied load corresponding to this drift was measured to be 35.8 kN by the load cell on the actuator. At the drift ratio of 0.56% in the first cycle of 0.75% target drift ratio, the initial yielding of the longitudinal reinforcement (reaching the yield strain) was recorded by the strain gauges located at the beam's critical sections shown in Fig. 3(a).

3.2 Standard brick infilled frame (SBF)

Standard brick infill frame was designed as comparison frame in order to compare its response against locked brick infill frame. The first damage was observed when the infill wall separated from the beam at a drift level of 0.20%. The applied load at this drift level was 96.3 kN. The first flexural cracks were observed at a story drift of 0.34%. The applied load measured at this drift level

Table 1 Damage states at different drift ratios and corresponding force levels measured for all specimens

Specimen	First separation		First diagonal crack		First flexural cracks		First yielding		Concrete spalling		Observed max. lateral load	
	Drift [%]	Load [kN]	Drift [%]	Load [kN]	Drift [%]	Load [kN]	Drift [%]	Load [kN]	Drift [%]	Load [kN]	Drift [%]	Load [kN]
BaF	-	-	-	-	0.28	35.8	0.56	57.3	2.00	93.0	2.50	100.9
SBF	0.20	96.3	0.40	120.0	0.34	116.2	0.67	129.0	2.00	107.3	1.50	137.4
LBF	0.20	55.8	0.25	67.8	0.35	68.6	0.75	85.2	2.00	84.4	3.00	97.5

Standard brick infilled frame

Locked brick infilled frame

+1.0 % drift ratio

+2.5% drift ratio

+3.5 % drift ratio

Fig. 4 Infilled frame states at different drift levels

was 116.2 kN. At the drift ratio of 0.67% in the first cycle of 0.75% target drift ratio, the initial yielding of the longitudinal reinforcement bar in the beam was recorded.

3.3 Locked brick infilled frame (LBF)

The first damage was observed when the infill wall separated from the beam at an inter-story drift level of 0.20%. The applied load at this drift level was 55.8 kN. The first cracks related to flexural behavior were observed at a story drift of 0.35%. The applied load was measured 68.6 kN. At maximum drift ratio in the first cycle of 0.75% target drift ratio, the initial yielding of the longitudinal reinforcement in the beam was recorded.

Table 1 summarizes observed damage states of the walls and structural system and corresponding force levels; in addition to these, first yielding of the reinforcing bars and observed maximum lateral load levels are also documented.

Fig. 4 shows the states of SBF and LBF specimens at different drift ratios for visual damage comparison on the infill walls. At high drift ratio levels, it is particularly apparent that LBF specimen suffers considerably less infill damage. At the end of the test at 3.5% drift ratio, bricks in the LBF specimen remained almost intact and only plaster cracks were observed whereas in the SBF specimen many bricks were lost due to diagonal forces.

4. Analysis of test results

The test results are compared with each other in terms of lateral strength and general behavior, lateral stiffness, and cumulative and relative energy dissipation characteristics. The advantages and drawbacks of different infill walls are also discussed.

4.1 Lateral strength and the general behavior of the specimens

The envelope curves of lateral load versus story drift responses obtained using test data for the BaF, SBF, and LBF specimens are presented in Fig. 5. Two sets of envelope curves for each RC frame are shown in the figure. Solid lines represent the envelope curves constructed from the data recorded during the first cycle of that specific target drift level (Yuksel *et al.* 2010), and the dashed lines represent the envelope curves constructed using the procedure outlined in FEMA-356 (2000) where the values at intersection points of the 1st cycle for the ith drift level, and the 2nd cycle for the (i-1)th drift level are used. These plots represent the lateral strength versus lateral drift capacities of each specimen subjected to the same displacement demand.

The effect of the standard brick infill can be seen clearly. By referring to Fig. 5 SBF specimen reaches to relatively high lateral load value whereas BaF and LBF specimens have lower lateral load values, this is particularly important for the LBF specimen since this frame behaves very similar in terms of lateral load capacity as the BaF specimen at higher drifts because in the locked brick wall there is no mortar connecting the brick units. At lower drift levels, different behavior of LBF and BaF is due to the fact that locked brick wall contributes to the lateral stiffness. The lateral load capacity of BaF increases approximately 15% when standard brick infills are used and almost no increase is observed in the case of LBF with respect to FEMA envelope curve procedure. A slight lower value in the lateral load capacity of LBF according to BaF specimen can be due to

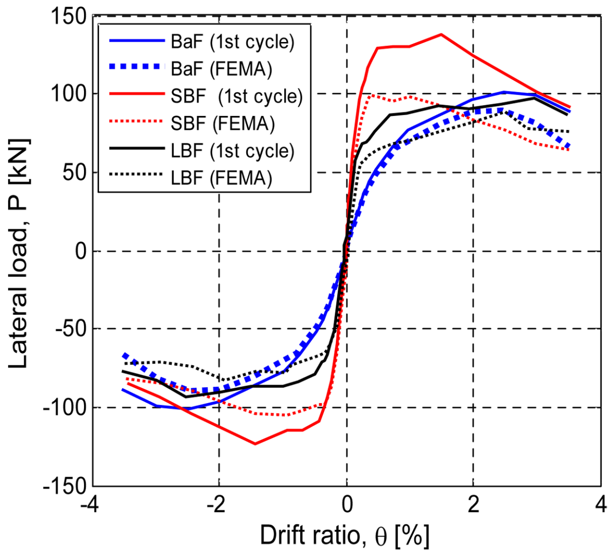

Fig. 5 Envelope curves for bare, standard brick infilled and locked brick infilled frames (solid-line from 1st cycle data; dashed-line from FEMA-356 prestandard procedure - design parameters and acceptance criteria)

Table 2 The observed ultimate strengths (1st cycle)

Specimen	Push [kN]	Pull [kN]
Bare frame	99.5	-100.0
Standard brick infilled frame	137.1	-123.4
Locked brick infilled frame	93.0	-93.4

material variability and different curing conditions. Results show that infill walls deteriorate quickly as the cycles progress within the same target drift level, and therefore it can be said that infill walls have very low ductility. It is seen that all the specimens reach to similar lateral load values beyond 2% drift ratio indicating that infill walls do not contribute to the ductility of RC frames at high drift levels. The ductility of the infill walls are considerably low which makes it important to consider in all structural performance evaluations. Table 2 summarizes the maximum strength values reached for the pushing and pulling directions separately, and in the same order ultimate base shear capacities are 99.5 kN, 137.1 kN, and 93.0 kN for the positive loading direction, respectively.

4.2 Lateral stiffness

The peak-to-peak lateral stiffness is defined as the slope of the line connecting the positive and negative peak values of a load-displacement cycle under consideration. Variations in the lateral stiffness values with respect to story drift are calculated at the third cycle of each drift ratio (i.e., target displacement) and are plotted in Fig. 6. As shown in the figure, the BaF specimen constitutes the lower bound in the stiffness degradation curves. For the BaF, SBF and LBF specimens, initial elastic lateral stiffnesses are 13.4 kN/mm, 71.4 kN/mm, and 39.2 kN/mm, respectively. In the elastic

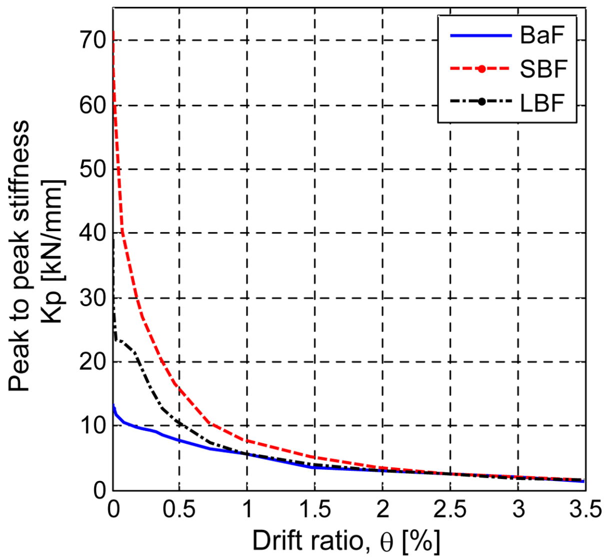

Fig. 6 Stiffness degradation behaviour of specimens

range, the stiffnesses of the SBF and LBF are 5.33 and 2.93 times larger than the corresponding stiffness of the bare frame (BaF), respectively. The LBF specimen has higher stiffness values at early stages of the loading but drops down to 23.5 kN/mm when story drift reaches to 0.028%. This sudden drop at the beginning of the test is due to passing the static friction threshold of locked bricks and the shear failure of the plaster. After that the stiffness starts decreasing once shear sliding starts within the infill wall and as the drift ratio increases the stiffness decreases further gradually. After about 2.0% drift level, similar stiffness degradation can be observed in all the specimens.

4.3 Energy dissipation capacity

The capacity of a structure to dissipate seismic input energy is a key measure of how it will perform under seismic action. The cumulative dissipated energy is defined as the sum of the area enclosed by each hysteresis loop at the same target drift level. The cumulative dissipated energy vs. story drift ratio plots are shown for all specimens in Fig. 7. Discontinuities seen at target drift levels are due to having three cycles at each drift level, therefore dissipated energy accumulates with each cycle at the same drift level. The lines between the target drift levels are added to increase the readability of the plots; otherwise they do not have any physical meanings. By referring to Fig. 7, it can be said that BaF specimen has the minimum energy dissipation capacity whereas SBF specimen has the highest. At 1.5% drift level where approximately the peak load levels were reached, SBF specimen dissipates 2.78 and 1.71 times more energy than BaF and LBF specimens, respectively.

Another energy dissipation measure called the relative energy dissipation ratio is also used. This ratio is defined in ACI 374.1-05 as the ratio of actual to ideal dissipated energy by a test specimen between specified drift ratio limits during reversed cyclic response. The same ratio can also be used to compare the energy dissipation performances of frame type specimens. The relative energy dissipation ratio (β_i) vs. (ith) drift ratio of the test specimens are given in Fig. 8, the details regarding β_i can be found in the above given reference.

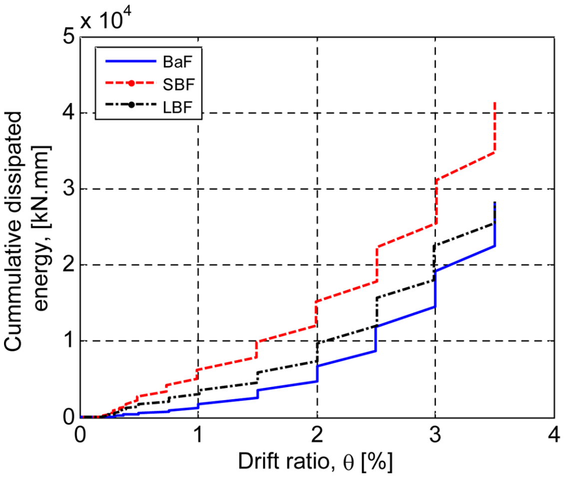

Fig. 7 The dissipated cumulative energy vs. drift ratio plots for all specimens

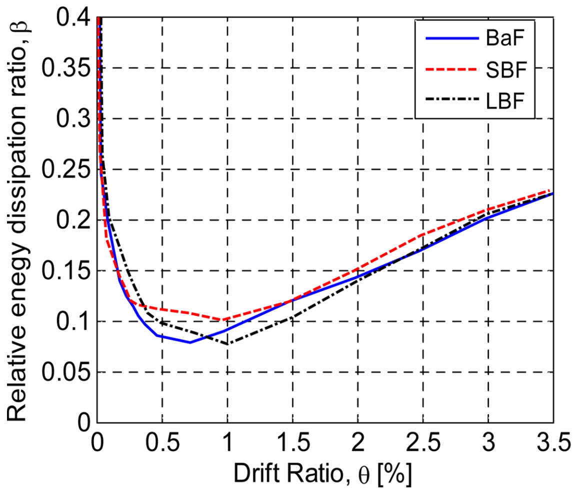

Fig. 8 Relative energy dissipation ratio (β) for the bare frame

The β_i ratios tend to decrease in the first several cycles. During the test, no damage was observed in these cycles. The system was in the elastic range. Once the cracks start to form, various energy dissipation mechanisms get activated and input energy is dissipated by the system which in return results in increase in β_i values. This trend can be seen clearly for all the specimens. Based on the ACI 374.1-05 report, the relative energy dissipation ratio calculated at ±3.5% drift ratio is recommended to be at least 12.5%. This criterion is satisfied for all the specimens. This is especially important for the LBF specimen since a new type of brick is used as infills and shows that acceptance criterion is satisfied. Moreover, very similar β_i trends are observed for all the specimens at different drift levels.

5. Conclusions

The presence of masonry infill walls affect the seismic behavior of framed building to a large extent. These effects are generally positive based on the type of masonry infilled used. Masonry infills increase global stiffness and strength of the structure. In this paper, three one bay-one storey RC frames with different masonry infill conditions are tested under cyclic loading. Results are presented in terms of force-interstory drift ratio envelope curves, lateral stiffness, cumulative and relative energy dissipation ratio plots. It is observed that

i. Standard brick infills do not increase the lateral load capacity of RC frames considerably within the results of FEMA-356 procedure. The lateral load capacity of bare frame increases approximately 15% with standard brick infills and almost no increase is observed when locked brick infills are used.

ii. Since the ductility of the standard brick infill wall is very low, lateral resistance contribution of this infill is almost negligible at high drift levels. For the locked brick infill wall, since the wall is free to deform with the frame, lateral strength do not change considerably. For all the specimens, similar story shear values are observed beyond 2% drift ratio.

iii. Locked brick infill suffers considerably less infill damage at high drift levels. At the end of the test at 3.5% drift ratio, bricks in the LBF specimen remained almost intact and only plaster cracks were observed whereas in the SBF specimen many bricks were lost due to diagonal forces.
iv. The cumulative energy dissipation capacity of the frames with both types of infill walls is higher than that of the bare frame. But this is due to reaching higher levels of lateral forces. For a better comparison of energy dissipation capabilities of the frames with different types of bricks, the relative energy dissipation ratios are calculated, and the results show that both types of bricks contribute more to the energy dissipation capacity of the frames at drift ranges between 0.5% and 1% drift. At higher drift levels, energy dissipation capacities for three different frames are similar.
v. Infill walls in general are not taken into account during the modeling phase of the structures, but it is a well known fact that they change the dynamic characteristics of the structures; in this paper it is shown that the locked brick infills change the initial lateral stiffness of the structure much less than the standard infills, therefore the modeled and the real structure will be more similar in terms of their dynamic characteristics, and the design will be more reliable.
vi. Locked brick infills change the lateral stiffness of RC frames considerably less compare to the standard infills; this attribute of the locked bricks has the potential in reducing the negative effects of vertical and lateral stiffness irregularities in structures caused by irregular layout of infill walls at different story levels.
vii. Locked brick infills preserved their in-plane stability from the start till the end of the test; indicating that the locked brick infills have an improved behavior in out-of-plane stability compare to the standard bricks. This may prove useful during a multi-axial earthquake shaking by lowering falling hazards of infill walls on people and therefore decreasing related injuries and fatalities. In the future, out-of-plane stability test should be performed to assess this behavior quantitatively at various limit states.
viii. Locked brick infills maintained their integrity up to very high drift levels (i.e., 3% and beyond) with sliding failure. This behavior may be used to develop engineered infilled reinforced concrete frames.

Analytical considerations will be discussed in a future paper in which mechanical properties and modeling parameters will be determined and a parametric study will be performed.

References

ACI Committee 374 (2005), *Acceptance Criteria for Moment Frames Based on Structural Testing and Commentary, ACI 374.1-05,* American Concrete Institute, Farmington Hills, Detroit, Michigan.

Aref, A.J. and Jung, W.Y. (2003), "Energy dissipating polymer matrix composite-infill wall system for seismic retrofitting", *J. Earthq. Eng.,* **129**(4), 440-448.

Dolsek, M. and Fajfar, P. (2001), "Soft storey effects in uniformly infilled reinforced concrete frames", *J. Earthq. Eng.,* **5**(1), 1-12.

Dolsek, M. and Fajfar, P. (2005), "Simplified non-linear seismic analysis of infilled reinforced concrete frames", *Earthq. Eng. Struct. D.,* **34**, 49-66.

FEMA-356 (2000), *Prestandard and Commentary for the Seismic Rehabilitation of Buildings*, Federal Emergency Management Agency, Washington, D.C.

Hashemi, A. and Mosalam, K.M. (2006), "Shake-table experiment on reinforced concrete structure containing masonry infill wall", *Earthq. Eng. Struct. D.,* **35**, 1827-1852.

Kakaletsis, D. (2009), "Analytical modeling of masonry infills with openings", *Struct. Eng. Mech.,* **31**(4), 499-520.

Klingner, R.E. and Bertero, V.V. (1976), *Infilled Frames in Earthquake-resistant Construction*, Rep. EERC 76-32, University of California, Berkeley.

Lagaros, N.D. and Geraki, M.A. (2008), "The effects of construction practices on the seismic performance of RC frames with masonry infills", *Struct. Eng. Mech.,* **28**(1), 69-88.

Ministry of Public Works and Settlement (2007), *Specification for Structures to be Built in Disaster Areas*, Turkey.

Mohammadi, M. and Akrami, V. (2010), "Application of frictional sliding fuse in infilled frames, fuse adjustment and influencing parameters", *Struct. Eng. Mech.*, **36**(6), 715-727.

Mohammadi, M., Akrami, V. and Ghazi, R.M. (2011), "Methods to improve infilled frame ductility", *J. Struct. Eng.,* **137**, 646-653.

Mondal, G. and Jain, S.K. (2008), "Lateral stiffness of masonry infilled Reinforced concrete (RC) frames with central opening", *Earthq. Spectra*, **24**(3), 701-723.

Perera, R., Gomez, S. and Alarcon, E. (2004), "Experimental and analytical study of masonry infill reinforced concrete frames retrofitted with steel braces", *J. Struct. Eng.*, **130**(12), 2032-2039.

Pujol, S. and Fick, D. (2010), "The test of a full-scale three-story RC structure with masonry infill walls", *Eng. Struct.,* **32**, 3112-3121.

Santhi, H.M., Knight, G.M.S. and Muthumani, K. (2005), "Evaluation of seismic performance of gravity load designed reinforced concrete frames", *J. Perf. Const. Facil.*, **19**(4), 277-282.

Sezen, H., Whittaker, A.S., Elwood, K.J. and Mosalam, K.M. (2003), "Performance of reinforced concrete buildings during the August 17, 1999 Kocaeli, Turkey earthquake, and seismic design and construction practice in Turkey", *Eng. Struct.,* **25**, 103-114.

Talaat, M. and Mosalam, K.M. (2009), "Modeling progressive collapse in reinforced concrete buildings using direct element removal", *Earthq. Eng. Struct. D.*, **38**(5), 609-634.

Tasnimi, A.A. and Mohebkhah, A. (2011), "Investigation on the behavior of brick-infilled steel frames with openings, experimental and analytical approaches", *Eng. Struct*., **33**, 968-980.

Ugurlu, M.A. (2011), "Cyclic characterization of locked and standard brick infilled reinforced concrete frames under quasi-static loading conditions: experimental and analytical work", MSc. Thesis, Graduate School of Natural and Applied Sciences, Dokuz Eylul University, Izmir, Turkey.

Yuksel, E., Ozkaynak, H., Buyukozturk, O., Yalcin, C., Dindar, A.A., Surmeli, M. and Tastan, D. (2010), "Performance of alternative CFRP retrofitting schemes used in infilled RC frames", *Constr. Build. Mater.*, **24**, 596-609.